ELSEVIER

Quaternary Science Reviews 27 (2008) 337–350

QSR

Holocene optimum events inferred from subglacial sediments at Tschierva Glacier, Eastern Swiss Alps

U.E. Joerin[a,*], K. Nicolussi[b], A. Fischer[c], T.F. Stocker[d], C. Schlüchter[a]

[a]*Institute of Geological Sciences, University of Bern, Baltzerstrasse 1, CH-3012 Bern, Switzerland*
[b]*Institute of Geography, University of Innsbruck, Innrain 52, A-6020 Innsbruck, Austria*
[c]*Institute for Meteorology and Geophysics, University of Innsbruck, Innrain 52, A-6020 Innsbruck, Austria*
[d]*Climate and Environmental Physics, Physics Institute, University of Bern, Sidlerstrasse 5, CH-3012 Bern, Switzerland*

Received 17 December 2006; received in revised form 25 October 2007; accepted 26 October 2007

Abstract

This study investigates the subglacial sedimentary archive at Tschierva Glacier, Eastern Swiss Alps. Subfossil wood remains found at the retreating glacier tongue indicate that their emergence results from recent transport from an upvalley basin. A confluence-basin-like structure was found to exist by georadar measurements underneath the present glacier. In combination with high resolution age determinations based on dendrochronology and radiocarbon dating it is implied that a retreated Tschierva Glacier allowed vegetation growth and sediment accumulation in that basin. Three periods of glacier recession were detected, which occurred around 9200 cal yr BP, from 7450 to 6650 cal yr BP and from 6200 to 5650 cal yr BP. These periods are called Holocene optimum events (HOE). Accordingly, an equilibrium line rise >220 m compared to the reference period from 1960 to 1985 was inferred from digital elevation models of former glacier extents. Since glacier mass balance depends on summer (June–July–August) temperature and precipitation, an equilibrium line altitude (ELA) rise of 220 m implies a summer temperature increase of about 1.8 °C assuming unchanged precipitation during the dated HOE. Alternative calculations point to probable temperature increase in a broad interval between $+1.0$ °C taking into account a precipitation change of -250 mm/a to $+2.5$ °C with $+250$ mm/a precipitation change, supporting earlier paleotemperature estimates. It is proposed that higher mean summer insolation caused a stronger seasonality during the mid-Holocene as compared to late Holocene conditions.

1. Introduction

A broadly stable Holocene climate is revealed by studies on oxygen isotopes as a proxy of annual temperature in Greenland ice cores (Johnsen et al., 1997) and northern Alpine lake sediments (von Grafenstein et al., 1999). However a growing number of studies (Mayewski et al., 2004 and references there) have demonstrated that climatic variations occurred repeatedly throughout the Holocene on a multi-centennial scale. Typically, a change to cooler conditions is associated with glacier advances and deposition of moraines. The impact of such events was previously reported by Denton and Karlén (1973) and since then in more detailed studies from many mountain ranges, e.g. in Scandinavia (Matthews et al., 2000, 2005; Nesje and Dahl, 2003), in North America (Calkin et al., 2001; Reyes and Clague, 2004; Miller et al., 2005), the Alps (Furrer, 1991; Nicolussi and Patzelt, 2000b). However, information is generally sparse on periods of glacier retreat, because subsequent glacier advances overrode smaller moraines resulting in a tendency to overestimate the frequency and magnitude of glacier advances. Additional information is archived in lake sediments, the analysis of which could help to overcome these difficulties (Dahl et al., 2003). For example, in the Alps, lake sediments have provided insights into the Holocene environmental conditions based on physical parameters (Leemann and Niessen, 1994), pollen (Tinner et al., 1996; Haas et al., 1998), tree-line studies (Tinner and Theurillat, 2003; Nicolussi et al., 2005) and chironomid assemblages (Heiri et al., 2003). Since the problem of identifying directly the extent of glacier retreat

*Corresponding author. Tel.: +41 443633155; fax: +41 443639744.
E-mail address: ujoerin@geo.unibe.ch (U.E. Joerin).

0277-3791/$ - see front matter © 2007 Elsevier Ltd. All rights reserved.
doi:10.1016/j.quascirev.2007.10.016

has persisted, the question of the full amplitude of Holocene glacier fluctuations remains open (Furrer, 1991). As a consequence, difficulties exist when glacier records are compared to other proxies or against the influence of forcing factors on longer time scales. Therefore, assessing glacier recessions, in particular the amplitude of glacier fluctuations is an important paleoclimate issue.

Alpine glaciers adapt their geometry, particularly glacier length, in response to variations in climate (Meier and Post, 1962; Oerlemans, 2005). Indeed, the ongoing rapid retreat of glaciers is well documented (WGMS, 1998; Dyurgerov, 2002) and is one of the consequences of recent global warming (IPCC and Climate Change, 2007). Field experiments and modelling studies have demonstrated that changes in glacier length mainly reflect variations in summer temperatures (Kerschner, 1997; Oerlemans, 2001; Vincent, 2002). Thus a recent study by Oerlemans (2005) demonstrated that measured glacier length records are an independent indicator of temperatures for the last 500 yr. The expansion further back in time requires reconstructions of glacier extent based on the geologic record. In the Alps, earlier studies concentrated on the dating of lateral or terminal moraines, which are associated with glacial advances during cold periods (Röthlisberger, 1986). Due to the discontinuous deposition of moraines such reconstructions are incomplete, in particular with regard to the extent and timing of glacier recessions. To overcome this problem, the discovery of wood and peat fragments associated with meltwater outburst events directed attention to the paleoclimate record of glacier fluctuations archived in subglacial basins (Nicolussi and Patzelt, 2000a; Hormes et al., 2001). Although the abundance of dating has improved the correlation of different records towards a general chronology (Joerin et al., 2006), the extent of glaciers during recessions has resisted a conclusive answer.

Here, we examine the Holocene recessions of Tschierva Glacier (eastern Swiss Alps) to provide a first constraint on minimum glacier extent that leads to a first-order estimate of the amplitudes of past glacier fluctuations. The exceptional discovery of well-preserved wood samples at Tschierva Glacier allows us to establish a dendrochronology of early Holocene events. We infer the area of original tree growth and subsequent subglacial preservation from georadar measurements and glacier bed topography in combination with stratigraphic evidence from the samples. Based on these results we reconstruct former glacier extents, which we use to calculate equilibrium line altitudes (ELA) in comparison to reference conditions from 1965 to 1985. Finally, the results are tested against independent reconstructions of paleotemperatures and discussed in the context of studies on natural climate variability during the Holocene.

2. Materials and methods

2.1. Characterisation of Tschierva Glacier

Tschierva Glacier is located on the north slope of the Bernina Massif, a part of the Eastern Swiss Alps (Fig. 1) where precipitation originates mainly from the south. The current climatic conditions are recorded at the nearby weather station of Sils (Begert et al., 2005), which is located at the border of Lake Silvaplana at 1798 m asl. The mean summer temperature (June–July–August, JJA) for the period from 1960 to 1985 is around 9.7 °C at Sils, which is extrapolated to 3.0 °C at the ELA of Tschierva Glacier (2820 m asl) using a lapse rate of −0.0065 °C/m. Similarly, the average precipitation (1960–1985) at Sils was

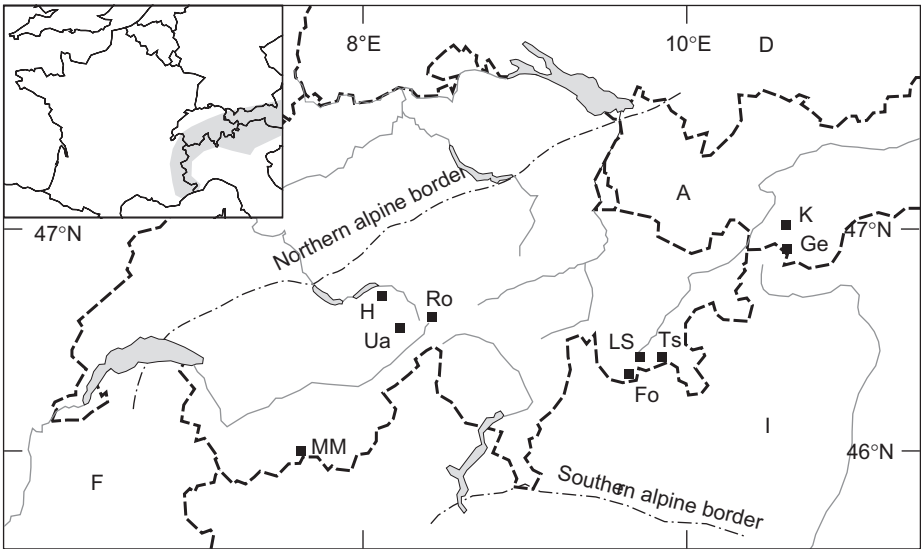

Fig. 1. Sketch map of the Swiss Alps and contiguous area. The location of Tschierva Glacier (Ts) and further locations mentioned in the discussion are marked by black squares: Fo = Forno Glacier, Ge = Gepatsch Glacier, H = Hinterburgsee, K = Kauner valley, LS = Lake Silvaplana with weather station Sils, MM = Mont Miné Glacier, Ro = Rhone Glacier, Ua = Unteraar Glacier.

978 mm/yr suggesting an extrapolated precipitation at the ELA of Tschierva Glacier around 1690 mm/yr (precipitation gradient of 0.7 mm/m).

The present situation at Tschierva Glacier is shown in Fig. 2a, where large and high lateral moraines are exposed since the glacier has retreated from its little ice age (LIA) extent. The last readvance from 1967 to 1987 built a small but well distinguishable terminal moraine (marked as 1985 in Fig. 2a) (Swiss Glaciological Commission, 1881–2002). After 1987, the glacier retreat has resulted in the new exposure of a forefield exhibiting till as well as bedrock areas. Striations on the exposed bedrock indicate former subglacial erosion. Outcrops near the main meltwater stream show a pattern of dominantly fluvial erosion (partly visible in Fig. 2b). Beside these areas, the metamorphic bedrock is covered by a thin unit of unconsolidated rocks consisting of a lodgement till that alternates with glaciofluvial deposits. The forefield is divided into an upper area on the gentle slope down to the 1985 moraine crest and the braided river system of the lower part. The discharge exhibits diurnal variations superimposed on a strong seasonal cycle. Irregular flood events are associated with individual weather systems, changes in the subglacial drainage system or combined to create meltwater outburst events (Röthlisberger and Lang, 1987). The distinct facies of a till unit is altered by fluvial processes in the vicinity of the glacier snout. Large parts of the upper forefield undergo cycles of sediment remobilisation (Fig. 2b) and redeposition including abrasional processes mainly associated with the occurrence of flood events. Sedimentation within a braided river system prevails in the lower part of Fig. 2a.

2.2. *Wood fragments in glaciofluvial sediments*

Although no trees grow in the modern catchment, wood fragments are found in the forefield of Tschierva Glacier. A detailed view of the upper part (Fig. 2b) illustrates the stratigraphic settings of our samples that are imbricated amongst boulders on the top of flood water sediments (A) or embedded in these glaciofluvial deposits (B). Rarely, samples were directly observed melting out at the front of the glacier tongue indicating englacial transport or being pressed onto the substratum near the ice front (Fig. 2c). Due to the lower slope angle, samples are also found on the top of occasionally flooded aggradations in the lower part of the forefield (Fig. 2a). In general, the number and locations of annual discoveries are related to the magnitude and frequency of outburst flood events.

Usually, wood samples are fragments of a log with dimensions less than 1 m long and 0.3 m wide, but some are as long as 8 m with diameters up to 0.8 m. Samples typically show abrasion, polished surfaces and imbrication of gravels indicating subglacial transport. Cross sections show that samples are sometimes deformed to an ellipsoid due to compression associated with subglacial burial. In general, the outer parts of the samples are unequally eroded and the

Fig. 2. The proglacial area of Tschierva Glacier (9.9.2004). (a, top) Wood fragments were found in the fluvial deposits marked with the grey boxes. Lateral moraines related to advances of the little ice age (LIA) and the early 1980s are marked as reference levels. (b, middle) Meltwater river at the snout of Tschierva Glacier. An imbricated wood fragment (A) has been deposited by a recent meltwater outburst. A tree log (B) embedded in fluvial gravel is covered by a 1 m thick lodgement till. (c, lower) Till units forming a moraine ridge at the right of a bedrock ridge have been recently exposed by the retreating ice margin. A deformed and partly abraded log (excavated on 12.7.2005) indicates subglacial transport.

bark is not preserved. Only a few sections still show remains of sapwood.

The interpretation of dates derived from organic samples collected in periglacial sediments depends on their history. Sources of uncertainty include different initial locations of wood, transport processes and the position of the wood at collection sites (Ryder and Thomson, 1986). Therefore, it is important to specify the history of the samples as given below in order to enable a conclusive interpretation.

2.3. Dendrochronology and radiocarbon dating

Dendrochronological analyses were used to determine the age of the wooden remains. As noted above, some samples displayed partially compressed sections of which some parts of the samples were excluded from dendrochronological analysis. The number of tree rings was estimated for such parts of a particular section.

Measurements of total ring width were carried out on the samples from the Tschierva Glacier forefield to a precision of 0.001 mm. At least two radii were investigated on each section. These measurements of different radii were averaged to a mean series for each sample. The tree-ring series of different samples, which originate from the same tree shown by dendrochronological analysis, were combined (Table 1). Only tree-ring series from uncompressed samples were used for dendrochronological synchronisation with the Alpine master chronology (Nicolussi et al., 2004). The Alpine master chronology is mainly based on subfossil samples from high altitude sites (>ca. 2000 m asl) in the western part of the Eastern Alps. The chronology covers continuously the last approx. 9000 yr. Floating chronologies are available for parts of the early Holocene (Nicolussi and Patzelt, 2000b). Dendrochronological crossdating of the Tschierva samples with the Alpine master chronology were carried out statistically and by visual control (Schweingruber, 1987).

Beside dendrochronological analysis we carried out radiocarbon dates on the Tschierva samples to improve the reliability of our chronology. For this purpose, samples were usually taken after the dendrochronological analysis was done and from a dendrochronologically defined position. The basis for determining the minimum lifespan of each sample (Table 1) was the number of counted rings, to which we added an estimate of the missing rings.

The measured conventional radiocarbon ages were calibrated applying the CALIB Rev 5.0 program (Stuiver and Reimer, 1993) in combination with the Intcal04 calibration dataset (Reimer et al., 2004). The corresponding lowest and highest limits of the 2-sigma standard deviation of the calibrated ages are reported. All values are rounded to the next decade (Table 2).

2.4. Georadar measurements

For this study, ice thickness data were collected with a lightweight GPR transmitter of Narod (Narod and Clarke, 1994) in combination with resistively loaded dipole antennas with an antenna half length of 15 m and a Fluke 105B oscilloscope (Span et al., 2005). The system operates at a frequency of 6.5 MHz, which is well suited for ice thickness measurements on temperate glaciers with a glacier bed consisting of bedrock or tills (Bogorodsky et al., 1985). The ice thickness was computed following the procedure of Span et al. (2005) assuming that the velocity of the radar signal in the ice is 168 m/μs (Robin, 1975). The distance between transmitter and receiver was 15 m. The winter snow layer with a thickness of less than 1 m at the time of the measurement was neglected. Positions were determined with a Garmin Summit GPS with a horizontal accuracy of approximately 5 m. Since the location where the radar signal is reflected on the steep or rough bedrock is not necessarily directly under the measurement point on the surface, the accuracy of this instrument is sufficient. The altitude was measured with the same GPS in the barometric mode and calibrated using a reference location near the glacier. The total vertical accuracy was determined to be within 5 m.

To reconstruct the glacier bed elevation, the calculated ice thickness was subtracted from the GPS measured ice surface elevation. The errors of the glacier bed reconstruction includes the GPS measurement error (<5 m), the conversion of the georadar signal to an ice depth (2%, which results in a typical uncertainty of <2 m at a depth of 100 m) and a geometrical error because of subvertical reflections assumed to be <10 m (equal to 10% at a depth of 100 m). Hence, the vertical resolution of this reconstruction is in the order of 5–15 m, but better than 17 m at an ice depth of 100 m. Due to subvertical reflections and GPS errors the horizontal resolution is assumed to be better than 15 m.

2.5. Glacier–climate relations expressed by equilibrium line altitudes

The ELA is a theoretical line where the net balance equals zero, and which separates the upper accumulation section from the lower ablation section on a glacier. The influence of climatic variations on glacier mass balance is reflected in changes of the ELA. Therefore, the ELA is thought to be a useful parameter to infer present and past climatic conditions (Kuhn, 1981; Dyurgerov, 2002). Several studies demonstrate a nonlinear relation between precipitation and ablation season temperature at the ELA. Based on a worldwide dataset from glaciers lying in mid to high latitudes Ohmura et al. (1992) found the equation

$$P_0 = 9\,T_0^2 + 296\,T_0 + 645, \quad (1)$$

where P_0 is winter accumulation plus summer precipitation (mm water equivalent per yr) at the ELA and T_0 is summer (JJA) temperature (°C) at the ELA. Following Ohmura et al. (1992) and assuming that (1) holds also in the past, a climatic change (ΔT and ΔP) at the ELA (altitude = z_0)

Table 1
Dendrochronological results of wood samples from Tschierva Glacier

Code	Tree species	Pith (y/n)	Tree-ring series (n)	Mean tree-ring width (mm)	Dendro date (yr BP)	Minimum lifespan (yr)
TSC-07	PICE	y	118	0.658	6815–6697	118
TSC-25	PICE	n	34	–[1]	–	c. 44
TSC-29	PICE	n	109	0.292	–	c. 139
TSC-102	PICE	n	115	0.237	6944–6830	c. 415
TSC-106	PICE	y	380	0.234	7223–6844	380
TSC-107	PICE	n	274	0.179	7067–6795	c. 434
TSC-108	PICE	n	131	0.872	6998–6868	c. 134
TSC-131	PICE	n	315	0.319	7134–6820	c. 565
TSC-133	PICE	n	73	0.398	6858–6813	c. 273
TSC-134	LADE	y	276	0.939	6148–5873	276
TSC-135	PICE	n	240	0.513	6993–6754	c. 400
TSC-136	PICE	y	102	0.656	5773–5672	102
TSC-137	PICE	n	173	0.342	6984–6812	c. 353
TSC-138	PICE	y	202	0.395	6070–5869	202
TSC-139	PICE	n	214	0.415	7035–6822	c. 334
TSC-142	PICE	n	240	0.458	7217–6978	c .290
TSC-143	PICE	n	177	0.162	7207–7031	c. 427
TSC-144	PICE	n	281	0.164	7129–6849	c. 381
TSC-45/159	LADE	y	163	0.574	6823–6661	163
TSC-146	PICE	n	89	1.278	6848–6760	c. 109
TSC-147	PICE	n	204	0.448	6895–6689	c. 324
TSC-148	PICE	n	289	0.159	7333–7045	c. 439
TSC-149	PICE	n	103	0.930	6866–6760	c. 173
TSC-150	PICE	n	147	0.470	–	c. 197
TSC-151	PICE	y	242	0.389	7061–6870	242
TSC-152	PICE	y	407	0.512	7164–6758	407
TSC-153	PICE	n	296	0.689	7062–6767	c. 346
TSC-154	PICE	n	206	0.698	6898–6693	c. 355
TSC-155	PICE	n	397	0.268	7247–6851	c. 462
TSC-156	PICE	n	63	1.291	6791–6729	c. 88
TSC-157	PICE	y	625	0.175	7444–6820	625
TSC-158	PICE	y	156	0.921	–	156
TSC-160	PICE	y	596	0.460	7424–6829	596
TSC-161	PICE	n	187	0.164	6925–6739	c. 337
TSC-162	PICE	y	179	0.601	6871–6693	179
TSC-163	PICE	n	288	0.414	7135–6787	c. 538
TSC-164	PICE	y	416	0.185	7294–6879	416
TSC-170	PICE	n	78	0.671	7176–7099	c. 228
TSC-171	PICE	n	440	0.576	7289–6850	c. 443
TSC-172	PICE	y	353	0.471	7123–6771	353
TSC-173	LADE	n	365	0.604	7000–6636	c. 370
TSC-174	PICE	n	76	0.846	–	c. 86
TSC-11/140	LADE	n	247	1.319	6157–5909	c. 267

Abbreviations: PICE = *Pinus cembra* L; LADE = *Larix decidua* Mill.; Pith y = yes, n = no; Dendro date = absolute years before 1950; c. = estimate of missing rings in addition to all counted rings.

causes a shift (Δz) of the equilibrium line to a different altitude z_1, where the new precipitation and temperature are related as given in Eq. (2):

$$\Delta P + (\partial P/\partial z)\,\Delta z = (\partial P/\partial T)_{zo}(\Delta T + (\partial T/\partial z)\,\Delta z), \qquad (2)$$

Where $\partial P/\partial z$ is the precipitation gradient, $(\partial P/\partial T)_{zo}$ is the derivative of Eq. (1) with the given P–T values at the ELA and $\partial T/\partial z$ is the temperature gradient. Therefore, this equation relates the climatic change (ΔT, ΔP) to the corresponding shift (Δz) of the ELA. Rearranging Eq. (2) for ΔT

$$\Delta T = -(\partial T/\partial z)\Delta z + (\Delta P + (\partial P/\partial z)\Delta z)/(\partial P/\partial T)_{z_o}, \qquad (3)$$

permits one to calculate a temperature change from a given ELA shift Δz and a precipitation change ΔP. Because linear approximations are used in Eq. (2) and (3), their application should be restricted to relatively small variations only.

Different approaches are used to determine former ELA which then allow us to calculate changes in ELA at different times and to infer variations of paleoclimatic conditions (Benn and Evans, 1998; Dahl et al., 2003). All methods rely on the fact that datable glacigenic sediments permit the reconstruction of specific parameters of a former glacier extent which is converted to a corresponding ELA (Meier, 1965; Furbish and Andrews, 1984). Here, the

Table 2
Radiocarbon dates of wooden remains at Tschierva Glacier

Code	Tree-ring series (*n*)	^{14}C sample (tree-ring series no.)	Lab. code	^{14}C age (yr BP)	Cal ^{14}C age (2σ) (yr BP)	Absolute age range of the ^{14}C sample (yr BP)
TSC-07	118	92–115	B-8552	5920±30	6840–6670	6724–6701
TSC-25	34	1–34	B-7627	8221±34	9300–9030	–
TSC-29	109	*	B-7628	5990±30	6910-6740	–
TSC-107	274	*	B-8300	6145±29	7160–6960	(7067–6795)#
TSC-108	131	*	B-8177	6044±29	6970–6800	(6998–6868)#
TSC-133	73	32–71	GrN-29540	5975±25	6880–6740	6827–6788
TSC-136	102	92–101	GrN-29541	5025±30	5890–5660	5682–5673
TSC-138	202	114–176	B-8553	5240±40	6180–5920	5957–5895
TSC-143	177	90–171	B-8554	6050±40	7000–6790	7118–7037
TSC-146	89	46–61	GrN-29542	5965±35	6890–6680	6803–6788
TSC-148	289	169–262	GrN-29543	6155±35	7160–6960	7165–7072
TSC-149	103	58–74	B-8555	6030±30	6950–6790	6809–6793
TSC-150	147	55–82	B-8556	6120±40	7160–6900	–
TSC-157	625	488–500	GrN-29544	6135±25	7160–6950	6957–6945
TSC-158	156	145–155	B-8557	5120±30	5830–5750	–
TSC-211	144	*	B-8312	5339±27	6260–6000	(6157–5909)#

Tree ring series are according to Table 1, and where possible, the material used for radiocarbon dating was expressed as tree ring number. * = no defined sampling. Labor code B = University of Bern, GrN = University of Groningen. 14-C age = conventional radiocarbon age before 1950 AD. Cal 14-C age includes the 2-sigma age range after calibration. Absolute age range denotes the calendar years before 1950 of the selected material based on dendrochronology using the calibrated age as a first estimate for the synchronisation procedure. # = age range of the whole tree-ring series.

following procedure was used to infer past climatic conditions and compare them with present conditions. The length of Tschierva Glacier[1] measured since 1943 exhibits a generally receeding trend during the 20th century, interrupted by a readvance from 1967 to 1987 (Swiss Glaciological Commission, 1881–2002). The extent of the terminal moraine ridge from the early 1980s is defined as 1985 reference level of near steady state, which is comparable to the reconstruction of the 1973 extent by (Maisch, 1992). Former glacier extents are determined based on the interpretation of maps or the zone of potential tree growth. Subsequently, the area per elevation of a specific glacier extent was calculated using ArcGis 9.0 and a digital elevation model (25 m grid) covering the Swiss Alps (Swisstopo, 2003a). The accumulation area ratio (AAR) method assuming a fixed value of 0.65 according to Maisch (1992) was used to determine an ELA corresponding to a specific glacier extent. This procedure yields similar results in comparison to the balance ratio method used with a ratio of two (Furbish and Andrews, 1984; Benn and Gemmell, 1997), because the main part of Tschierva Glacier exhibits almost a constant area per elevation distribution.

3. Results

3.1. Chronology

We analysed 43 samples from wood remains found on the forefield of the Tschierva Glacier. The wood species of most samples is *Pinus cembra* L.; the other sections are from *Larix decidua* Mill. trees. Up to approximately 600 yr long tree-ring series could be carried out on the samples investigated.

Fig. 3 shows ages and lifespans of wood samples indicating a smaller glacier than today during the periods called Holocene optimum events (HOE). According to radiocarbon and dendrochronological results, the wooden remains analysed originate from three different time periods (Table 1 dendrochronology and Table 2 radiocarbon dating and calibration).

Only one sample containing less than 40 tree-rings dates around 9300/9000 cal yr BP, which is the oldest HOE at the Tschierva Glacier. Most of the wooden remains date between approx. 7450 and 6650 cal yr BP. The combined individual tree-ring series covers a time period of more than 800 yr. Remains of sapwood on the sections of the youngest trees (Fig. 3) indicate a synchronous death of at least these trees shortly after 6630 cal yr BP, which was probably caused by a glacier advance. The third HOE begins around 6200 cal yr BP. The distribution of the samples indicates a likely glacier advance with two phases (around 5800 and 5650 cal yr BP, respectively). However, the tongue of the Tschierva Glacier retreated behind the actual position during these periods of tree growth.

3.2. Determination of the tree growth area

The wood fragments are derived from a thin layer of fluvially reworked till deposits on top of bedrock. This stratigraphic position and the nearby exposed bedrock with glacigenic striations indicate that the wood fragments are not in situ but transported by ice and meltwater. Therefore,

[1]Data are online available at: http://glaciology.ethz.ch/messnetz/index.html

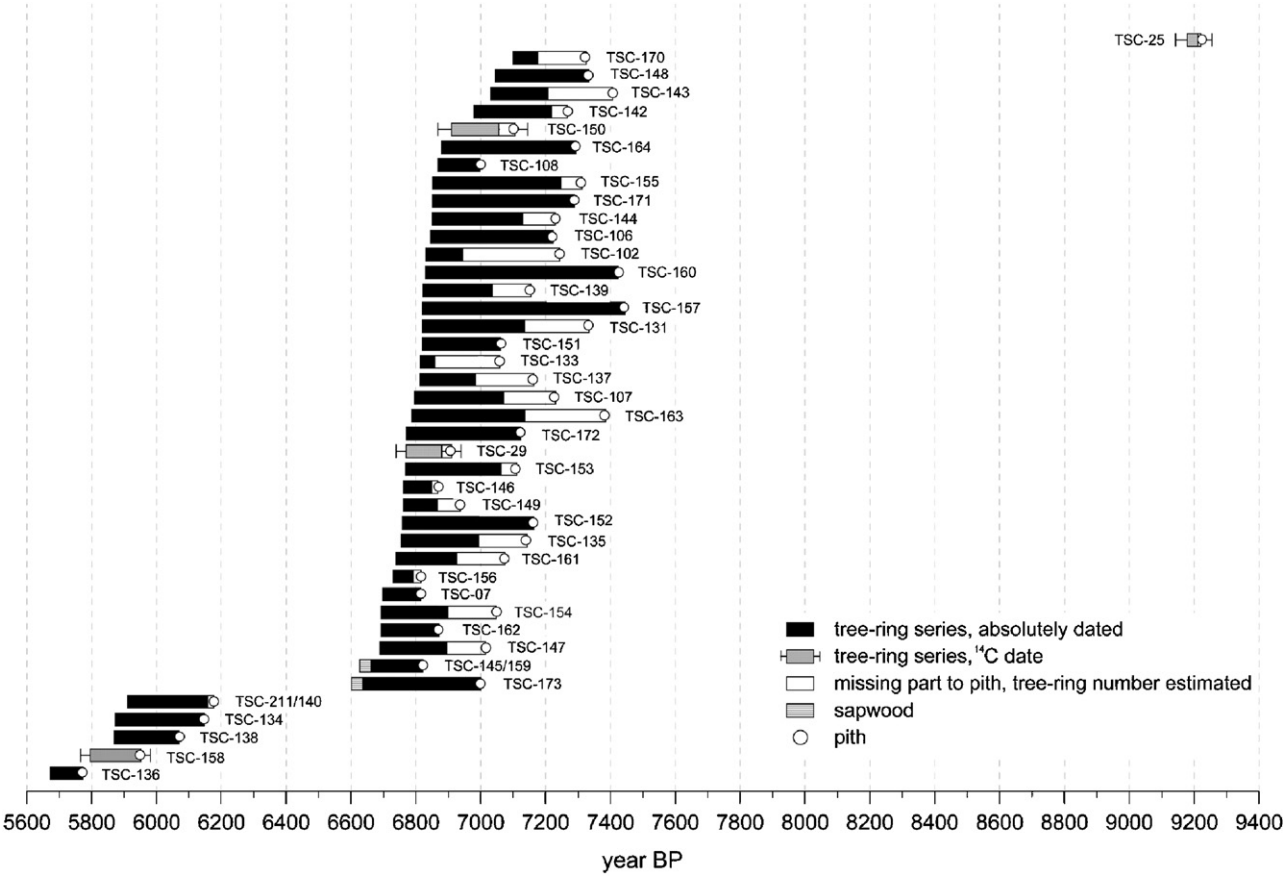

Fig. 3. Ages and lifespans of wood fragments: dendrochronological age determinations with lifespans based on counted rings. Some dates rely on calibrated radiocarbon ages (black bars indicate 2-sigma probability interval of calibration). A major recession, called Holocene optimum event (HOE), started around 7450 cal yr BP lasting for 800 yr. Few trees germinated after 6900 cal yr BP, while vice versa most trees were embedded after 6900 cal yr BP. A hiatus between the last ring observed (virtual tree death) and the true tree death must be regarded because of abrasion of some outer rings. It is interpreted that a glacier advance could have overridden and embedded a large number of the samples after 6900 cal yr BP. Tree growth during a second HOE occurred from 6200 cal yr BP until 5650 cal yr BP.

deposits with embedded wood must exist further upvalley under the present glacier. In order to examine this area in more details, the glacier bed was reconstructed using georadar. Fig. 4a illustrates the elevation of the ice surface measured by GPS, which show a general down-wasting of the tongue since 1990, the datum of the underlying reference map. The depth of ice between the surface and the first reflector is displayed in Fig. 4b. The elevation of the glacier bed is obtained from the surface elevation subtracted by the measured ice depth. The signal of the first reflector represents the boundary between glacier ice and the glacier bed, which may consist of bedrock or sediments. Due to surface crevasses, the lateral parts show a poor coverage of measurements, which mainly follow along a central flowline. The results from the upper part indicate the presence of an area with a confluence basin-like structure (red circle in Fig. 4c). The shallow ice depth in the lower part, marked as "barrier" in Fig. 4c, is interpreted as an area with small scale obstacles, which are comparable to the Forno Glacier forefield (Joerin et al., 2006) or the Rhone Glacier terminus (Zahno, 2004).

Fig. 5 shows a profile along a line with dense measurements (Fig. 4c). The ice surface was reconstructed for the survey date 7 April 2005) and a 1990 ice surface was drawn for comparison based on the topographical map (Swisstopo, 2003b). The bedrock steeply dips from up-stream (2700 m asl) down into the plateau at an elevation of 2300 m asl. With regard to the confluence of the three upper parts of Tschierva Glacier, the detected glacier bed is interpreted as a confluence basin, which we believe is partially infilled with sediment. Comparable situations frequently exist in the Alps, in particular at the Rhone Glacier (Zahno, 2004). The basin is terminated by a wide and flat barrier (Riegel), which continues as a gentle slope down to the present tongue and the position of the wood finds. Because the wood samples are embedded in glaciofluvial gravel on a slope, and because the potential of subglacial erosion increases with slope (Sugden and John, 1976), it is concluded that our findings are not in situ and do not originate from an original slope position.

Conversely, sedimentation prevails in flat or ascending parts. Therefore, accumulated sediments including wood fragments will be preferentially preserved in small-scale

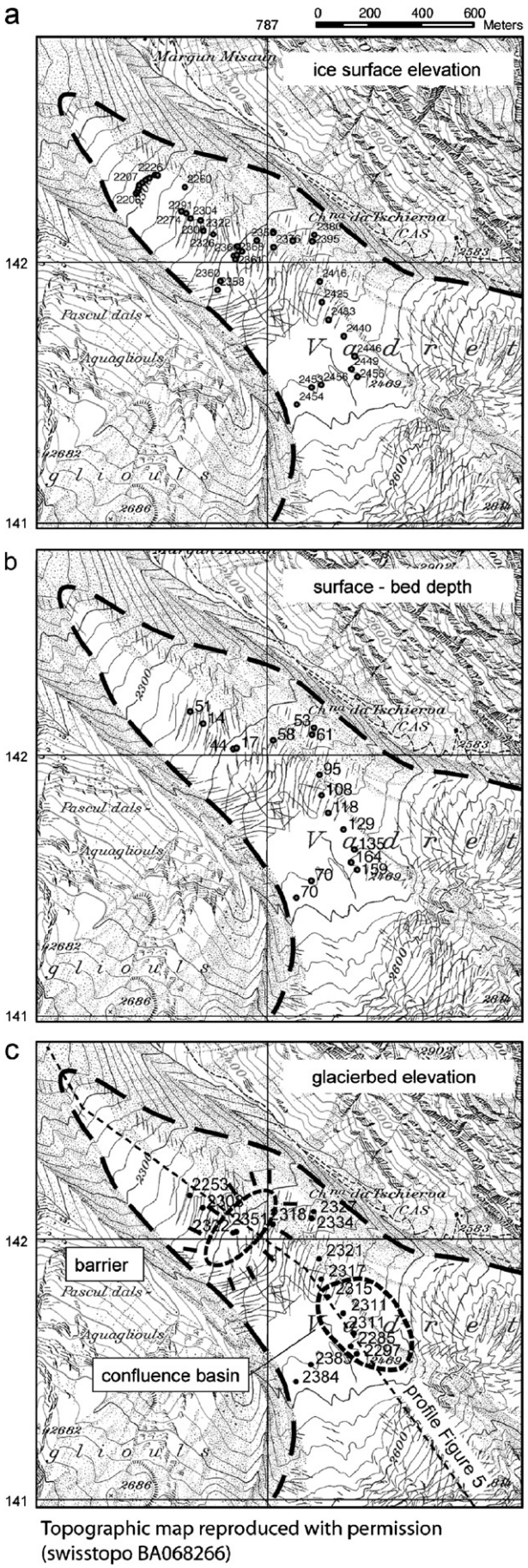

basins on the upper side of the barrier, which is gently ascending. Nevertheless, a small fraction of sediment was likely transported to the glacier tongue by freeze-on layers initiated during the last readvance or by the meltwater system (Röthlisberger and Lang, 1987; Benn and Evans, 1998).

After a zone of potential preservation of organic material had been detected, we sought to define the possible locations of former tree growth with respect to the former glacier extent. The upper limit was approximated at 2500 m asl resulting from the 1980 tree line at 2350 m asl, adding 170 m for higher tree lines in the early Holocene (Tinner et al., 1996; Nicolussi et al., 2005). The steep slopes of the surrounding area suggest that horizontal transportation of wood is unlikely. The potential area of tree growth is limited to the main valley occupied by the present glacier. Wood input to lateral sediments by avalanches could influence our interpretation (Ryder and Thomson, 1986), but is excluded for our samples at the Tschierva Glacier because any wood deposited on the glacier would be transported down to the glacier tongue before embedding into sediments at the valley bottom. In addition, tree-ring analyses imply that many trees grew under constant conditions for over 300 yr, which is not the case in a typical avalanche path. Typical indications of avalanche-affected wood, like reaction wood, eccentricity of the tree-ring growth, frequent abrupt growth reductions (Casteller et al., 2007), are missing.

Taken together, the information on sample morphology, synchrony of the tree-ring series, clustering of tree deaths, etc. corroborate our proposed growth and embedding mechanisms. Therefore, the embedding into sediments at the inferred position seems to be possible only under a scenario with a glacier terminating at the upper border of the basin (approx. at 2450 m asl) or, most likely at even higher elevations.

3.3. Tschierva Glacier extent reconstructions

We reconstruct the extent of a receded Tschierva Glacier under the assumptions that the trees grew in the detected basin and that the glaciers terminated at the upper border of the basin or at higher elevations (Fig. 6). We divide the glacier into three parts because of the separating bedrock ridges in the upper catchment. The cumulative area per

Fig. 4. Results of the georadar measurements and the glacier bed reconstruction. The dashed line outlines the 1990 glacier extent. (a) Part of Tschierva Glacier (Swiss Grid coordinates are labelled at the border) with GPS measured ice surface elevations plotted on the topographic map from 1990. The lowest points mark the glacier tongue terminating at 2207 m asl on 07.04.05. (b) points with georadar ice thickness measurements (values = depth (m)); (c) Inferred glacierbed elevations at specific measurement points calculated from ice surface data (a) and georadar ice depths (b), for details see text). The interpreted structures are plotted as dashed lines. The central part of the cross section of Fig. 5 is along the light dashed line as marked in Fig. 4c. Topographic map reproduced with permission (swisstopo BA068266).

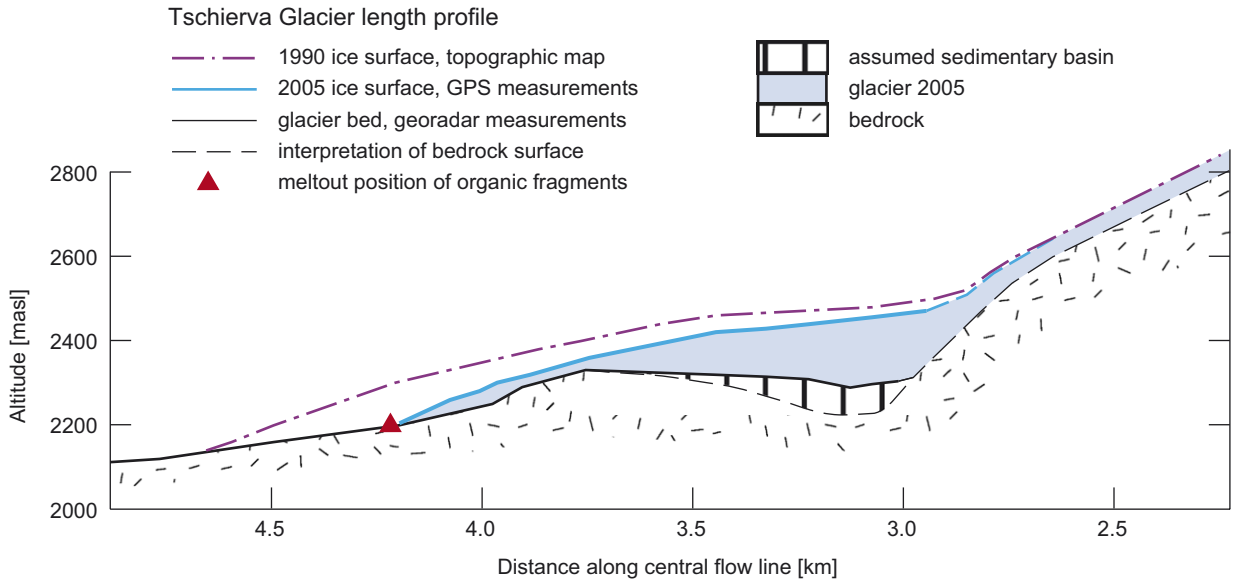

Fig. 5. Cross section along the line marked in Fig. 6. Reconstructions of the ice surface based on GPS measurements for 2005 and on map interpretations for the 1990 extent. The lower boundary of the assumed basin infill was approximated (for details see text) while the upper boundary (equal to the glacierbed) was reconstructed by georadar measurements. The upside icefall is based on the 1990 map.

elevation was calculated for each part of the upper catchment separately. We determined the ELAs for each part by applying the rule of an AAR equal to 0.65 This shows that the glaciation of the central part defines the relevant ELA at an altitude of 3040 m asl in order to maintain an ice free basin. The glaciered area shown in Fig. 6 represents a maximum length of the glacier for the periods fulfilling the previous requirements, which are called HOE. This reconstruction is compared to the reconstructed glacier extent known from the 1985 reference position as well as the LIA, which both are preserved as moraine ridges (given in Fig. 2a). The corresponding ELAs were calculated to be at (rounded to 10 m) 3040 m asl for the HOE, 2820 and 2710 m asl for the 1985 reference level and the LIA, respectively, using the area elevation distribution and an AAR = 0.65. Fig. 7 displays the cumulative area distribution of Tschierva Glacier for the three Holocene climatic conditions.

Assuming that minor oscillations in the order of ± 50 m may occur more frequently, the mean ELA during a HOE would be even at a higher elevation than the previously determined ELA of 3040 m asl. Hence, we conclude that our reconstruction of HOEs suggests a *minimum* rise of the ELA of 220 ± 20 m allowing tree growth in an ice-free basin.

4. Discussion

4.1. Characteristics of HOE in the Swiss Alps

Subfossil logs embedded in glaciofluvial sediments at the Tschierva Glacier snout indicate periods of smaller glacier extent than at present. The best documented HOE occurred from 7450 to 6630 cal yr BP while indications exist for further HOEs approximately around 9.2 kyr BP and from 6200 to 5650 cal yr BP. These results support investigations on recessions at Unteraar Glacier and Mont Miné Glacier for the same periods (Hormes et al., 2001), at Pasterze Glacier in the Austrian Alps (Nicolussi and Patzelt, 2000a) at Forno Glacier (Joerin et al., 2006) and the chronology of glacier retreat during a major part of the Atlantic summarised by Grove (1988). Due to numerous samples and accurate dating, the two main recession periods at Tschierva Glacier (7450–6630 cal yr BP and 6200–5650 cal yr BP) are determined in unprecedented detail in comparison to other sites and thus help refine the chronology and amplitude of Alpine glacier fluctuations.

An earlier compilation of glacier fluctuations (Maisch et al., 1999) based on moraine datings and pollen profiles indicated that a similar glacier extent to that of 1980 occurred between 7600 and 5900 cal yr BP and around 9000 ± 100 cal yr BP. While the general timing is in a rough agreement with our newly proposed HOE chronology, the latter contains more information on germination periods and interpreted advances with high accuracy. Our chronology differs to that proposed by Röthlisberger (1986) and Röthlisberger and Schneebeli (1979), because the latter rely on interpretations of few minimum or maximum ages from dated paleosoils which are subject to methodological discussions (Matthews, 1997; Hormes et al., 2004).

Previous estimates of the amplitudes of recessions are based on sparse information (Maisch et al., 1999, p.52). A general ELA rise was estimated in the order of 50 m above the 1985 reference position during periods with no indications for glacier advances. Our results suggest a revised ELA rise in the order of 220 m during HOEs. It is noted that the ELA rise during HOEs was derived by a well-defined (standard) procedure for glacier

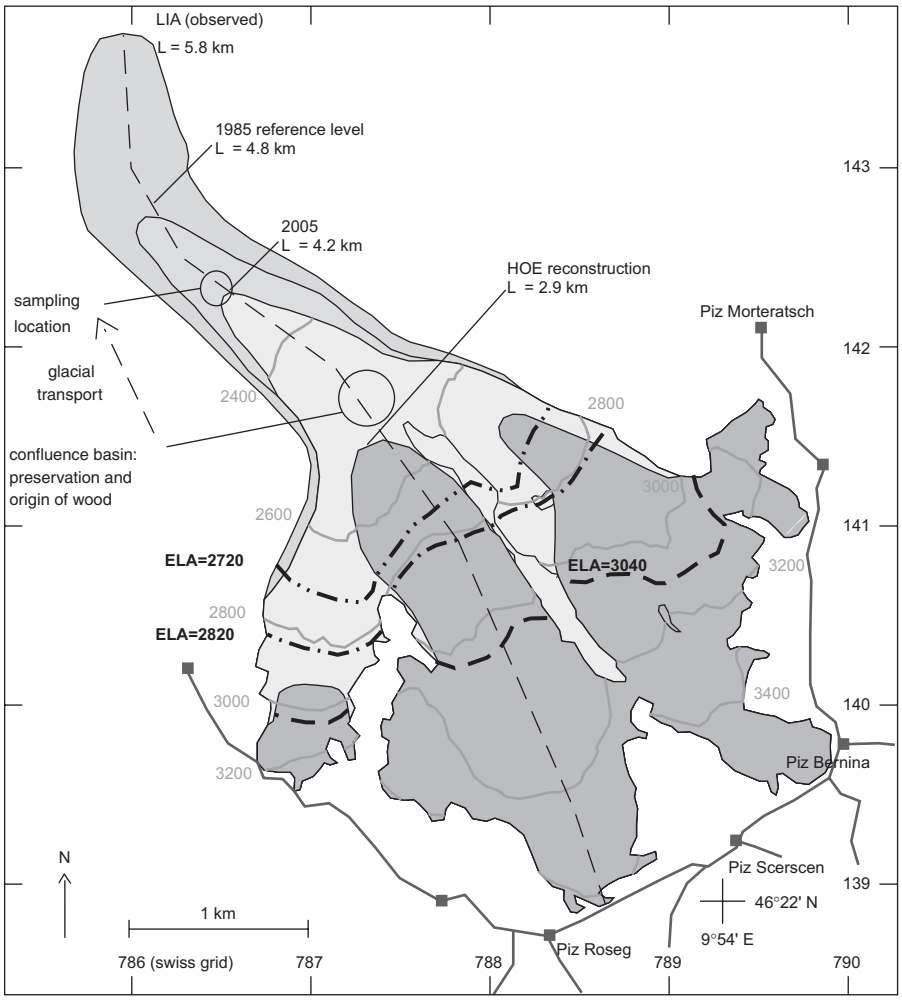

Fig. 6. Reconstructed surface extents at Tschierva Glacier and their corresponding length and equilibrium line altitudes (ELA) for the little ice age (LIA), the 1985 reference level and Holocene optimum events (HOE). The detailed procedure to reconstruct the minimum ELA during the HOE is given in the text. The ELAs shown here correspond to the values resulting from the calculated area-elevation distributions from Fig. 7. The cross section shown in Fig. 5 follows the lower part of the central flowline, which begins at the top of the glacier (distance = 0 km). The length from top to the glacier terminus is displayed for the LIA-event (length = 6.9 km), the 1985 reference position (4.9 km) and the HOEs (<2.9 km). The wood remains were found in front of the present glacier terminus (length = 4.1 km in 2005) with indications of glacial transport. Ticks at the border denote Swiss Grid coordinates (1 km spaced).

reconstruction. As a consequence, some discrepancies between our results and earlier studies may be explained by different definitions of the term "glacier recession", in particular to unquantified ELA rises and the glaciological significance of the dated wood samples.

Support for warmer conditions and higher ELAs comes from different archives, in particular from proxies derived from lake sediments or peat bogs. An analysis of sediments from Lake Silvaplana located in an adjacent valley (7 km from the study site) with a close climatic relation suggested a virtually ice-free upper catchment from 9400 to 3300 conv. yr BP (Leemann and Niessen, 1994). This implies also an ELA rise in the order of 100 m based on reconstructed ELAs and scenarios for increased temperatures from Maisch (1992) and Maisch et al. (1999). A similar impact on the ELA fluctuations in the nearby Tschierva Glacier catchment is expected, which is in agreement with our results.

Alpine glacier fluctuations and the changes of the tree line are controlled mainly by summer temperature variations, which are consistent on a regional scale. Evidence for generally higher tree lines was found in the Swiss Alps by Tinner and Theurillat (2003), whilst Nicolussi et al. (2005) reported that the highest trees found in mires in the Kauner valley (Central Austrian Alps) grew from 7450 to 6300 cal yr BP up to 165 m higher than the 1980 tree line. Further, there is evidence for a very high tree line starting shortly after 9200 cal yr BP and for a depression around 8500 cal yr BP. Again, the oldest Tschierva sample dated to 9200 cal yr BP coincides with the start of a tree line rise.

4.2. Paleoclimatic implications

Generally higher summer temperatures in the order of 1 °C during the early and mid Holocene were reported by Heiri et al. (2003) based on chironomid assemblages from

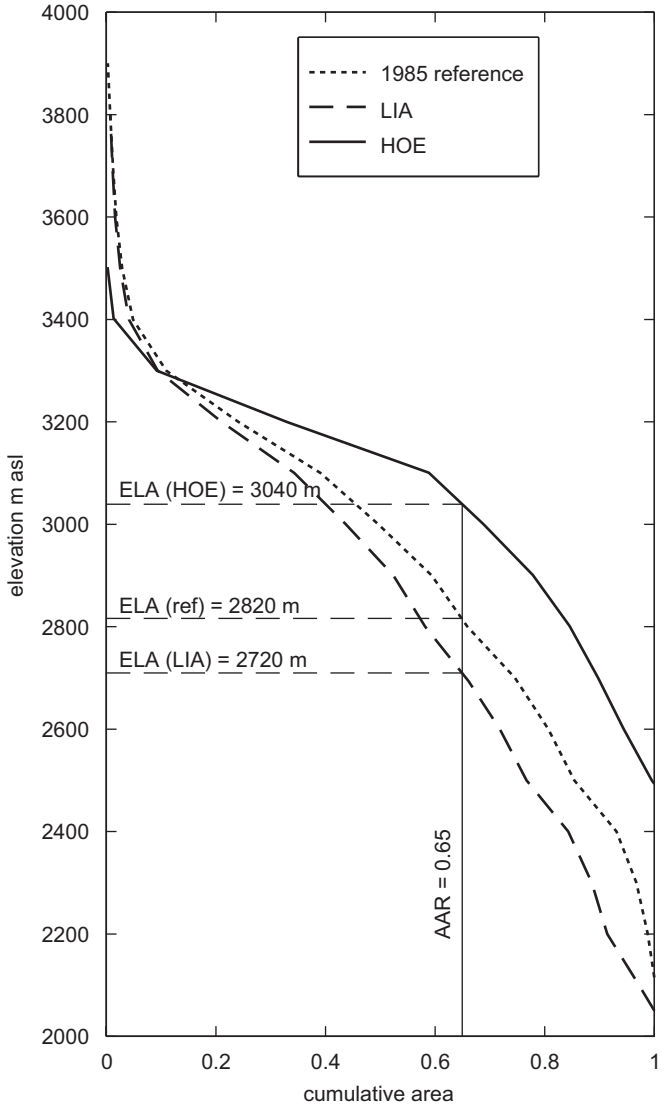

Fig. 7. Calculated curves of the cumulative area for three reconstructions of Tschierva Glacier: 1985 reference level, little ice age (LIA) and Holocene optimum events (HOE). The equilibrium line altitude (ELA) is determined where the accumulation area ratio equals 0.65 yielding the following values: ELA for 1985 reference = 2820 m asl; ELA for LIA = 2720 m asl; ELA for HOE = 3040 m asl.

sediments of Lake Hinterburgsee located at the northern alpine front. Regarding single values of the unsmoothed curve the peaks exceed a 1.5 °C increase in summer (June) temperature around 7600, 7400, 6300, 4800 cal yr BP coinciding partly with the HOEs. Based on the previously determined ELA rise of 220 m and an assumed sensitivity of the ELA around 140 m/°C (Kerschner, 1997; Kuhn, 1981), a simple temperature calculation supports an increase of 1.6° during the multi-century long HOEs. This climatic signal derived from glacier recessions coincides with the highest tree lines in the Austrian Alps 7500–6800 yr ago (Nicolussi et al., 2005), which also indicates warmer summer temperatures. Hence, several studies located at different altitudes within the Alps indicate that summer temperatures were >1 °C warmer at that time.

Despite this general consensus on periods of warmer than present summer temperatures, differences exist due to different assumptions on paleo-temperature calculations. Moreover, an ELA shift depends on both precipitation and temperature changes. In order to constrain the implications of our reconstructed minimum ELA rise of 220 m, a set of different scenarios was used to calculate the difference of paleo-temperatures against the reference conditions of the ELA (1960–1985) by applying Eq. (3). The ELA shift was kept constant (values listed in Table 3), but precipitation was prescribed to differ from the reference conditions (given in Section 2.1). We were therefore able to examine the influence of precipitation and temperature associated to the given ELA shift. The scenarios show that the ELA shift of +220 m with an assumed precipitation change of +250 mm/a would imply an synchronous increase in summer temperature of about +2.5 °C. On the other hand, a precipitation reduction of 250 mm/a results in a much smaller increase of +1.0 °C for the summer temperature, while the same precipitation amount as at present yields a medium temperature increase of 1.8 °C (Table 3).

4.3. Glacier response to changing insolation and seasonality

This study and data by others indicate that higher summer temperatures (Heiri et al., 2003; Tinner and Theurillat, 2003; Nicolussi et al., 2005) occurred during the first part of the Holocene, but mean annual temperatures remained almost unchanged (von Grafenstein et al., 1999). These climatic conditions are interpreted to reflect changes in insolation (Berger, 1978), which probably caused a stronger seasonality at this time. Ganopolski et al. (1998) reported that higher summer temperatures and a change in vegetation cover resulted from a mid-Holocene simulation with prescribed changes in insolation compared to a control run with present conditions. Because the sensitivity of glacier mass balance depends on summer temperatures (Oerlemans, 2001) our reconstructed glacier recessions may reflect partly a long term trend of changed seasonality and insolation but also a superimposed signal of multi-century scale fluctuations (Joerin et al., 2006). The influence of each part cannot be quantified with the available data. Recent summaries of glacier fluctuations in Norway (Matthews et al., 2005), Baffin Island (Miller et al., 2005) and British Columbia (Menounos et al., 2004) indicate, that glaciers were generally shorter during the early Holocene and started to advance more frequently after 6 kyr BP, before peaking with the LIA. Such a similar trend of glacier fluctuations from several locations in the Northern Hemisphere seems to support a strong influence of summer insolation on seasonality and in turn on glaciers during the Holocene.

Because of a change in seasonality glaciers, may have fluctuated far above the present extent during previous

Table 3
Different climatic scenarios of Holocene optimum events (HOEs) and the parameters used to calculate the change of paleo-temperatures as compared to the reference conditions (1960–1985)

Calculated scenarios for Holocene optimum events (HOE)						
Scenario	Prescribed values					Result
	dP*(mm)	ELA shift (m)	$\partial P/\partial z$ (mm/m)	$\partial T/\partial z$ (°C/m)	T_o** (°C)	ΔT (°C)
A	0	220	0.7	−0.006	3.0	+1.8
B	250	220	0.7	−0.006	3.0	+2.5
C	−250	220	0.7	−0.006	3.0	+1.0

All scenarios base on the same ELA shift of +220 m and constant gradients of temperature and precipitation as well as the same climatic reference conditions T_0 and P_0 at the reference ELA.*ΔP = precipitation change, P = winter snow accumulation + summer precipitation after Ohmura et al. (1992). **T_o = mean summer temperature (JJA) at the reference ELA.

periods. That could partly explain the difficulty in finding an impact of the 8.2 ka event in the glacier record in the Alps except for Kerschner et al. (2006). Further research investigating these questions will help to quantify the dynamics of past Holocene climate changes and century scale climate variability. Moreover, independent estimates of Holocene annual precipitation variability will improve past temperature reconstructions based on glacier fluctuation records.

5. Conclusions

Our results indicate smaller glaciers than the 1985 reference level on at least three occasions during the early and mid-Holocene in accordance with earlier studies on Holocene glacier recessions (Orombelli and Mason, 1997; Nicolussi and Patzelt, 2000a; Hormes et al., 2001). The timing of glacier recessions and readvances was inferred from dendrochronological and radiocarbon dating. The results indicate that a first HOE started around 9200 cal yr BP and further periods lasted from 7450 to 6650 cal yr BP and from 6200 to 5650 cal yr BP. Tree-ring analysis implies a glacier advance shortly after 6630 cal yr BP and probably an advance with two phases around 5800 and 5650 cal yr BP, respectively. The events are dated with high accuracy and improve the existing chronology of glacier fluctuations derived by radiocarbon dating at six Swiss glaciers (Joerin et al., 2006). Our chronology implies that the total duration of HOEs during the Atlantic lasted as long as 1400 yr, more than twice as long as previous studies suggested (Röthlisberger, 1986). Glacier recessions for the same periods are also reported from Norway (Matthews et al., 2005), Baffin Island (Miller et al., 2005) or British Columbia (Menounos et al., 2004).

Stratigraphic, geomorphological and glaciological observations pinpoint to a source area of former wood growth in small upvalley basins. Such structures are confirmed by georadar measurements and exist underneath the present glacier at an altitude around 2300 m asl. The position of former tree growth restricts the extent of Tschierva Glacier during the HOE. Accordingly, the calculation of a former ELA suggests a local ELA at elevations above 3040 m asl or a rise in ELA >220 m compared to the 1985 reference for periods as long as 800 yr. Therefore, the range of Holocene ELAs may exceed a total amplitude of 320 m resulting from the Holocene extremes of an ELA depression around 100 m for the LIA and a 220 m rise for the HOE.

The summer (JJA) temperature during each HOE is calculated to have increased by +1.8 °C under the assumptions of an upward ELA shift of 220 m and no change in precipitation (based on a P–T-ELA model after Ohmura et al. (1992)). The periods of smaller glaciers than present agree with the results of biotic proxies (Tinner et al., 1996; Heiri et al., 2003; Nicolussi et al., 2005). Since mean annual temperatures remained almost unchanged during the mid-Holocene (von Grafenstein, et al., 1999) it is suggested that changes in insolation mainly caused an enhanced seasonality with higher summer temperatures at that time. As a consequence, the Tschierva Glacier advances after 6630 cal yr BP and around 5800 and 5650 cal yr BP represent centennial scale glacier fluctuations which probably occurred superimposed on a multi-millennial trend of generally shorter glaciers during the Atlantic.

Acknowledgements

We acknowledge the long-term support of the Bern Radiocarbon Lab by the Swiss National Science Foundation, and the careful sample processing and dating by R. Fischer and M. Möll. We thank A. Thurner for her precision and patience with the laborious dendrochronological measurements. This research has been supported by the Austrian Science Fund (FWF, Grant P15828 EX*PICE* to Kurt Nicolussi). Many friends helped with the field work and with critical discussions improving an earlier draft of this manuscript. We acknowledge the reviewer's critical suggestions and the support of the editorial office.

References

Begert, M., Schlegel, T., Kirchhofer, W., 2005. Homogeneous temperature and precipitation series of Switzerland from 1864 to 2000. International Journal of Climatology 25, 65–80.

Benn, D.I., Gemmell, A.M.D., 1997. Calculating equilibrium line altitudes of former glaciers by the balance ratio method: a new computer spreadsheet. Glacial Geology and Geomorphology.

Benn, D.I., Evans, D.J.A., 1998. Glaciers and Glaciation. Wiley, London, New York, Arnold.

Berger, A.L., 1978. Long-term variations of daily insolation and Quaternary climatic changes. Journal of the Atmospheric Sciences 35, 2362–2367.

Bogorodsky, V.V., Bentley, C.R., Gudmandsen, P.E., 1985. Radioglaciology. D. Reidel Publishing Company.

Calkin, P.E., Wiles, G.C., Barclay, D.J., 2001. Holocene coastal glaciation of Alaska. Quaternary Science Reviews 20, 449–461.

Casteller, A., Stöckli, V., Villalba, R., Mayer, A.C., 2007. An Evaluation of dendroecological indicators of Snow Avalanches in the Swiss Alps. Arctic, Antarctic and Alpine Research 39, 218–228.

Dahl, S.O., Bakke, J., Lie, O., Nesje, A., 2003. Reconstruction of former glacier equilibrium-line altitudes based on proglacial sites: an evaluation of approaches and selection of sites. Quaternary Science Reviews 22, 275–287.

Denton, G.H., Karlén, W., 1973. Holocene climatic variations-their pattern and possible cause. Quaternary Research 3, 155–205.

Dyurgerov, M.B., 2002. Glacier Mass Balance and Regime: Data of Measurements and Analysis (Occasional Paper 55). Institute of Arctic and Alpine Research, University of Colorado, Boulder.

Furbish, D.J., Andrews, J.T., 1984. The use of hypsometry to indicate long-term stability and response of valley glaciers to changes in mass transfer. Journal of Glaciology 30, 199–211.

Furrer, G., 1991. 25000 Jahre Gletschergeschichte. Naturforschende Gesellschaft in Zürich, Zürich.

Ganopolski, A., Kubatzki, C., Claussen, M., Brovkin, V., Petoukhov, V., 1998. The influence of vegetation–atmosphere–ocean interaction on climate during the mid-Holocene. Science 280, 1916–1919.

Grove, J.M., 1988. The Little Ice Age. Methuen, London, United Kingdom.

Haas, J.N., Richoz, I., Tinner, W., Wick, L., 1998. Synchronous Holocene climatic oscillations recorded on the Swiss Plateau and at Timberline in the Alps. The Holocene 8, 301–309.

Heiri, O., Lotter, A.F., Hausmann, S., Kienast, F., 2003. A chironomid-based Holocene summer air temperature reconstruction from the Swiss Alps. The Holocene 13, 477–484.

Hormes, A., Müller, B.U., Schlüchter, C., 2001. The Alps with little ice: evidence for eight Holocene phases of reduced glacier extent in the Central Swiss Alps. The Holocene 11, 255–265.

Hormes, A., Karlen, W., Possnert, G., 2004. Radiocarbon dating of Palaeosol components in moraines in Lapland, northern Sweden. Quaternary Science Reviews 23, 2031–2043.

IPCC, 2001. In: Solomon, S., et al. (Eds.), Climate Change, The Physical Science Basis. Contribution of Working Group I to the Fourth Assessment Report of the Intergovernmental Panel on Climate Change, Cambridge University Press, Cambridge.

Joerin, U.E., Stocker, T.F., Schlüchter, C., 2006. Multicentury glacier fluctuations in the Swiss Alps during the Holocene. The Holocene 16,5, 697–704.

Johnsen, S.J., Clausen, H.B., Dansgaard, W., Gundestrup, N.S., Hammer, C.U., Andersen, U., Andersen, K.K., Hvidberg, C.S., DahlJensen, D., Steffensen, J.P., Shoji, H., Sveinbjornsdottir, A.E., White, J., Jouzel, J., Fisher, D., 1997. The delta O-18 record along the Greenland Ice Core Project deep ice core and the problem of possible Eemian climatic instability. Journal of Geophysical Research—Oceans 102, 26397–26410.

Kerschner, H., 1997. Statistical modelling of equilibrium-line altitudes of Hintereisferner, central Alps, Austria, 1859-present. Annals of Glaciology 24, 111.

Kerschner, H., Hertl, A., Gross, G., Ivy-Ochs, S., Kubik, P.W., 2006. Surface exposure dating of moraines in the Kromer valley (Silvretta Mountains, Austria)-evidence for glacial response to the 8.2 ka event in the Eastern Alps? The Holocene 16 (1), 7–15.

Kuhn, M., 1981. Climate and glaciers. Sea Level, Ice and Climatic Change. IAHSPubl. No. 131.

Leemann, A., Niessen, F., 1994. Holocene glacial activity and climatic variations in the Swiss Alps: reconstructing a continuous record from proglacial lake sediments. The Holocene 4, 259–268.

Maisch, M., 1992. Die Gletscher Graubündens, Zürich.

Maisch, M., Wipf, A., Denneler, B., Battaglia, J., Benz, C., 1999. Die Gletscher der Schweizer Alpen. Gletscherhochstand 1850, Aktuelle Vergletscherung, Gletscherschwund-Szenarien. vdf Hochschulverlag AG, Zürich.

Matthews, J.A., 1997. Dating problems in the investigation of Scandinavian Holocene glacier variations. In: Frenzel, B. (Ed.), Glacier Fluctuations During the Holocene. Gustav Fisher Verlag, Stuttgart.

Matthews, J.A., Dahl, S.O., Nesje, A., Berrisford, M.S., Andersson, C., 2000. Holocene glacier variations in central Jotunheimen, southern Norway based on distal glaciolacustrine sediment cores. Quaternary Science Reviews 19, 1625–1647.

Matthews, J.A., Berrisford, M.S., Dresser, P.Q., Nesje, A., Dahl, S.O., Bjune, A.E., Bakke, J., John, H., Birks, B., Lie, O., Dumayne-Peaty, L., Barnett, C., 2005. Holocene glacier history of Bjørnbreen and climatic reconstruction in central Jotunheimen, Norway, based on proximal glaciofluvial stream-bank mires. Quaternary Science Reviews 24, 67–90.

Mayewski, P.A., Rohling, E.E., Curt Stager, J., Karlen, W., Maasch, K.A., David Meeker, L., Meyerson, E.A., Gasse, F., van Kreveld, S., Holmgren, K.U., 2004. Holocene climate variability. Quaternary Research 62, 243–255.

Meier, M.F., 1965. Glaciers and climate. In: Wright, H.E. (Ed.), The Quaternary of the United States. Princeton University Press, Princeton, NJ.

Meier, M.F., Post, A.S., 1962. Recent variations in mass net budgets of glaciers in western North America. IAHS Publ. No. 58.

Menounos, B., Koch, J., Osborn, G., Clague, J.J., Mazzucchi, D., 2004. Early Holocene glacier advance, southern Coast Mountains, British Columbia, Canada. Quaternary Science Reviews 23, 1543–1550.

Miller, G.H., Wolfe, A.P., Briner, J.P., Sauer, P.E., Nesje, A., 2005. Holocene glaciation and climate evolution of Baffin Island, Arctic Canada. Quaternary Science Reviews 24, 1703–1721.

Narod, B.B., Clarke, G.K.C., 1994. Miniature high-power impulse transmitter for radio-echo sounding. Journal of Glaciology 40, 190–194.

Nesje, A., Dahl, S.O., 2003. Glaciers as indicators of Holocene climate change. In: Mackay, A.W., Battarbee, R.W., Birks, H.J.B., Oldfield, F. (Eds.) Global Change in the Holocene. Arnold, London, UK, 2003.

Nicolussi, K., Patzelt, G., 2000a. Discovery of early-Holocene wood and peat on the forefield of the Pasterze Glacier, Eastern Alps, Austria. The Holocene 10.2, 191.

Nicolussi, K., Patzelt, G., 2000b. Untersuchungen zur holozänen Gletscherentwicklung von Pasterze und Gepatschferner (Ostalpen). Zeitschrift für Gletscherkunde und Glazialgeologie 36, 1–87.

Nicolussi, K., Lumassegger, G., Patzelt, G., Pindur, P., Schießling, P., 2004. Aufbau einer holozänen Hochlagen-Jahrring-Chronologie für die zentralen Ostalpen: Möglichkeiten und erste Ergebnisse. Innsbrucker Jahresbericht 2001/2002. Innsbrucker Geographische Gesellschaft, Innsbruck.

Nicolussi, K., Kaufmann, M., Patzelt, G., van der Plicht, J., Thurner, A., 2005. Holocene tree-line variability in the Kauner Valley, Central Eastern Alps, indicated by dendrochronological analysis of living trees and subfossil logs. Vegetation History and Archaeobotany, 221–234.

Oerlemans, J., 2001. Glaciers and Climate Change. A.A. Balkema, Lisse.

Oerlemans, J., 2005. Extracting a climate signal from 169 Glacier records. Science 308, 675–677.

Ohmura, A., Kasser, P., Funk, M., 1992. Climate at the equilibrium line of glaciers. Journal of Glaciology 38, 397.

Orombelli, G., Mason, P., 1997. Holocene glacier fluctuations in the Italian alpine region. In: Frenzel, B. (Ed.), Glacier Fluctuations During the Holocene. Gustav Fisher Verlag, Stuttgart.

Reimer, P., Baillie, M., Bard, E., Bayliss, A., Beck, J., Bertrand, C., Blackwell, P., Buck, C., Burr, G., Cutler, K., Damon, P., Edwards, R., Fairbanks, R., Friedrich, M., Guilderson, T., Hughen, K., Kromer, B.,

McCormac, F., Manning, S., Ramsey, C.B., Reimer, R., Remmele, S., Southon, J., Stuiver, M., Talamo, S., Taylor, F., Plicht, J.v.d., Weyhenmeyer, C., 2004. IntCal04 Terrestrial Radiocarbon Age Calibration, 0–26 cal kyr BP. Radiocarbon 46, 1029–1058.

Reyes, A.V., Clague, J.J., 2004. Stratigraphic evidence for multiple Holocene advances of Lillooet Glacier, southern Coast Mountains, British Columbia. Canadian Journal of Earth Sciences 41, 903–918.

Robin, G., 1975. Velocity of radio waves in ice by means of a bore-hole interferometric technique. Journal of Glaciology 15, 151–159.

Ryder, J.M., Thomson, B., 1986. Neoglaciation in the southern Coast Mountains of British Columbia: chronology prior to the late Neoglacial maximum. Canadian Journal of Earth Sciences 23, 273–287.

Röthlisberger, F., Schneebeli, W., 1979. Genesis of lateral moraine complexes, demonstrated by fossil soils and trunks; indicators of postglacial climatic fluctuations. In: Schluechter, C. (Ed.), Moraines and Varves; Origin, Genesis, Classification. A.A. Balkema, Rotterdam, Netherlands.

Röthlisberger, H., Lang, H., 1987. Glacial hydrology. In: Gurnell, A.M., Clark, M.J. (Eds.), Glaciofluvial Sediment Transfer. Wiley, New York.

Röthlisberger, F., 1986. 10000 Jahre Gletschergeschichte der Erde. Sauerländer, Aarau.

Schweingruber, F.H., 1987. Tree Rings: Basic Applications to Dendrochronology. Kluwer, Dordrecht.

Span, N., Fischer, A., Kuhn, M., Massimo, M., Butschek, M., 2005. Radarmessungen der Eisdicke österreichischer Gletscher, Band I: Messungen 1995 bis 1998. Österreichische Beiträge zur Meteorologie und Geophysik 33.

Stuiver, M., Reimer, P.J., 1993. Extended C-14 Data-Base and Revised Calib 3.0 C-14 Age Calibration Program. Radiocarbon 35, 215–230.

Sugden, D.E., John, B.S., 1976. Glaciers and Landscape a Geomorphological Approach. Arnold, London.

Swiss Glaciological Commission, 1881–2002. The Swiss Glaciers. Laboratory of Hydraulics, Hydrology and Glaciology (VAW) of ETH Zürich, Zürich.

Swisstopo, 2003a. DEM 25-Digital Elevation Model.

Swisstopo, 2003b. Topographical Map 1:25000.

Tinner, W., Theurillat, J.P., 2003. Uppermost limit, extent, and fluctuations of the timberline and treeline ecocline in the Swiss Central Alps during the past 11,500 years. Arctic Antarctic and Alpine Research 35, 158–169.

Tinner, W., Ammann, B., Germann, P., 1996. Treeline fluctuations recorded for 12,500 years by soil profiles, pollen, and plant macrofossils in the Central Swiss Alps. Arctic and Alpine Research 28, 131–147.

Vincent, C., 2002. Influence of climate change over the 20th Century on four French glacier mass balances. Journal of Geophysical Research—Atmospheres 107.

von Grafenstein, U., Erlenkeuser, H., Brauer, A., Jouzel, J., Johnsen, S.J., 1999. A mid-European decadal isotope-climate record from 15,500 to 5000 years BP. Science 284, 1654–1657.

WGMS, 1998. Fluctuations Of Glaciers 1990–1995. IAHS (ICSI)–UNEP–UNESCO, Paris.

Zahno, C., 2004. Der Rhonegletscher in Raum und Zeit: neue geometrische und klimatische Einsichten. Zürich, ETH Zürich.